

PRODUCTION OF CHARGED VECTOR BOSONS (X-MESONS) BY LEPTONS IN THE COULOMB FIELD OF NUCLEI

V. V. SOLOV'EV and I. S. TSUKERMAN

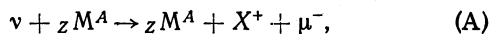
Submitted to JETP editor December 6, 1961

J. Exptl. Theoret. Phys. (U.S.S.R.) **42**, 1252-1259 (May, 1962)

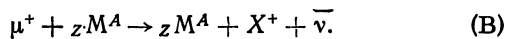
The cross sections (I) and (II) are calculated in the lowest order in weak and electromagnetic interactions. The expressions obtained are then employed to calculate the total cross sections for processes (A) and (B) by the Weizsäcker-Williams method. Curves of the cross section for X-meson production on the ${}_{26}\text{Fe}^{56}$ nucleus vs. the incident lepton energy, from the threshold up to 100 BeV, are presented for X-meson masses of 0.6 mp, 1.0 mp, and 1.4 mp.

It is known that a weak four-fermion interaction cannot be regarded as local within the framework of perturbation theory when the momentum transfer is large. In this connection, various authors have attempted to describe weak interaction as a nonlocal interaction of fermion currents through an intermediate vector boson,^[1] a particle with lifetime $\tau < 10^{-17}$ sec and mass κ exceeding the K-meson mass.

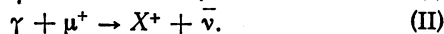
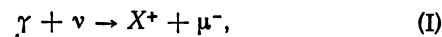
Several recent theoretical papers dealt with effects which, if confirmed experimentally, could serve as an argument for or against the existence of such a particle. The most convincing would be experiments on the direct production of the X meson. The simplest among these, as indicated by Pontecorvo and Ryndin,^[2] would be an experiment in which an X meson is produced by a neutrino in the Coulomb field of the nucleus,



since this experiment would not be accompanied by reactions caused by strong and electromagnetic interactions. A formula for the cross section of this process at large neutrino energies is contained in the paper delivered by Lee at the Rochester Conference of 1960.^[3] Ebell and Walker^[4] considered the "inverse" of reaction (A)



The purpose of the present paper is a detailed calculation of the total cross section σ_ν and σ_μ of processes (A) and (B), so as to make more precise the results of Lee and Yang^[3] and of Ebell and Walker.^[4] In Secs. 1 and 2 we calculate $\sigma_{\gamma+\nu}$ and $\sigma_{\gamma+\mu}$ for the reactions



In Sec. 3 we derive expressions for the cross sections σ_ν and σ_μ , using the covariant formulation of the Weizsäcker-Williams method^[5] and a very simple form factor of the "stepped" type. Plots of the cross sections of processes (A) and (B), calculated from the experimental distribution of the charge in the nucleus, are presented in Sec. 4 for the nucleus ${}_{26}\text{Fe}^{56}$ in the energy interval from threshold to 100 BeV.

1. CROSS SECTION OF THE PROCESS (I)

The Lagrangian of the interaction between leptons and the X meson has the form^[6]

$$L = f \bar{u}_\mu \gamma_\alpha (1 + \gamma_5) u_\nu \varphi_\alpha + \text{Herm. adj.}, \quad (1)$$

where u_μ and u_ν — Dirac spinors of the muon and neutrino, φ — wave function of the X meson, $f^2 = G\kappa^2/\sqrt{2}$ ($G = m_p^{-2} \times 10^{-5}$ — Fermi interaction constant, m_p — proton mass, and $\hbar = c = 1$).

In the lowest order in the weak and electromagnetic interactions, the matrix element T of process (I), represented by the diagrams of Fig. 1, is

$$T = -ief \frac{(2\pi)^4 \delta^4(k+p'-p-q)}{2\sqrt{\omega_k \omega_q}} \times e_\mu^{(\lambda)} e_\rho^{(\nu)} \bar{u}_\mu(\mathbf{p}) T_{\mu\rho} (1 + \gamma_5) u_\nu(\mathbf{p}'), \quad (2)$$

$$T_{\mu\rho} = (\Gamma_\mu)_{\rho\sigma} \frac{\delta_{\sigma\alpha} - \kappa^{-2} t_{1\sigma} t_{1\alpha}}{t_1^2 - \kappa^2} \gamma_\alpha + \gamma_\mu \frac{1}{t_2 - m} \gamma_\rho. \quad (3)$$

Here m — muon mass, ϵ_μ and ϵ_ρ — photon and X-meson polarization 4-vectors, $e^2/4\pi \equiv \alpha = 1/137$, $(\Gamma_\mu)_{\rho\sigma}$ — vertex part, describing the electromagnetic interaction of the X meson:^[7]

$$(\Gamma_\mu)_{\rho\sigma} = -(q_\mu + t_{1\mu}) \delta_{\rho\sigma} + t_{1\sigma} \delta_{\mu\rho} + q_\rho \delta_{\mu\sigma} + g (k_\sigma \delta_{\mu\rho} - k_\rho \delta_{\mu\sigma}), \quad (4)$$

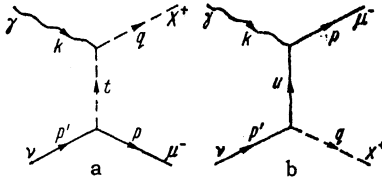


FIG. 1. Feynman diagrams of process (I); k, p', p and q —4-momenta of the photon, neutrino, μ^- meson and X meson, respectively; $t \equiv t_1 = q - k = p' - p$, $u \equiv t_2 = p - k = p' - q$.

where g —total gyromagnetic ratio for the X meson.

The matrix element (2) can be simplified by using the Dirac equation for the muon and neutrino, and the relations $e_{\mu}^{(\lambda)} k_{\mu} = 0$, $\epsilon_{\rho}^{(\nu)} q_{\rho} = 0$:

$$T_{\mu\rho} = \frac{-2q_{\mu}\gamma_{\rho} + g(\hat{k}\delta_{\mu\rho} - \hat{k}_{\rho}\gamma_{\mu})}{t_1^2 - \kappa^2} + \frac{2p_{\mu} - \gamma_{\mu}\hat{k}}{t_2^2 - m^2} \gamma_{\rho}. \quad (5)$$

In this expression we have neglected the terms $\sim m^2/\kappa^2$. It is easy to verify that the matrix elements in (3) and (4) are gauge-invariant.

The cross section $\sigma_{\gamma+\nu}$ of reaction (I) with longitudinally polarized neutrino, averaged over the photon polarizations and summed over the muon and X-meson polarizations, is

$$\sigma_{\gamma+\nu} = \frac{\alpha G}{4\sqrt{2}} \frac{\kappa^2}{s^2} \int \frac{dt^2}{s^2} \left(\delta_{\rho\sigma} - \frac{q_{\rho}q_{\sigma}}{\kappa^2} \right) Q_{\rho\sigma}, \quad (6)$$

$$Q_{\rho\sigma} = \text{Sp} [T_{\mu\rho} (1 + \gamma_5) \hat{p}' \gamma_4 T_{\mu\sigma}^+ \gamma_4 \hat{p}], \quad (7)$$

$$s = k + p' = p + q.$$

Integrating between the limits

$$t^2 |_{min}^{max} = \frac{1}{2} [(\kappa^2 - s^2 + m^2) \pm \sqrt{(s^2 - \kappa^2 + m^2)^2 - 4s^2 m^2}], \quad (8)$$

we obtain after simple calculations

$$\sigma_{\gamma+\nu} = \frac{\alpha G}{2\sqrt{2}} \left\{ \left[(g-2)^2 + (4-g^2) \frac{\kappa^2}{s^2} - \frac{8\kappa^4}{s^4} + \frac{8\kappa^6}{s^6} \right] \ln C \right. \\ \left. + \left[\frac{4\kappa^2}{s^2} - \frac{8\kappa^4}{s^4} + \frac{8\kappa^6}{s^6} \right] \ln D + \sqrt{\left(1 - \frac{\kappa^2}{s^2} + \frac{m^2}{s^2} \right)^2 - \frac{4m^2}{s^2}} \right. \\ \left. \times \left[\frac{1}{4} g^2 + 7g - 7 - \frac{1}{4} (g-2)^2 \frac{\kappa^2}{s^2} + \frac{8\kappa^4}{s^4} \right] \right\}; \quad (9)$$

$$\ln C = \ln \left[\frac{(s^2 + \kappa^2 - m^2) + \sqrt{(s^2 + m^2 - \kappa^2)^2 - 4s^2 m^2}}{(s^2 + \kappa^2 - m^2) - \sqrt{(s^2 + m^2 - \kappa^2)^2 - 4s^2 m^2}} \right], \\ \ln D = \ln \left[\frac{(s^2 + m^2 - \kappa^2) + \sqrt{(s^2 + m^2 - \kappa^2)^2 - 4s^2 m^2}}{(s^2 + m^2 - \kappa^2) - \sqrt{(s^2 + m^2 - \kappa^2)^2 - 4s^2 m^2}} \right]. \quad (10)$$

In (9) we neglected in the square brackets terms containing m^2/s^2 in the first and higher powers, since $m^2 \ll \kappa^2$.

At energies much higher than the threshold of reaction (1) ($\kappa^2 \ll s^2$), we obtain from (9) and (10) the following asymptotic formula

$$\sigma_{\gamma+\nu} = \frac{\alpha G}{2\sqrt{2}} \left\{ (g-2)^2 \ln \frac{s^2}{\kappa^2} + \left[\frac{1}{4} (g-2)^2 + 8(g-1) \right] \right\}. \quad (11)$$

2. CROSS SECTION OF PROCESS (II)

We now consider the process (II), which is the “inverse” of (I) and is represented by the diagrams of Fig. 2. The expressions for T , $T_{\mu\rho}$, and $Q_{\rho\sigma}$ corresponding to these diagrams are obtained from (2)–(5) and (7) by making the substitutions

$$p \rightarrow -p_+, \quad p' \rightarrow -p_-, \quad t_1 \rightarrow t'_1 \equiv t, \quad t_2 \rightarrow t'_2 \equiv -s', \\ \bar{u}_{\mu}(p) \rightarrow \bar{v}_{\mu}(-p_+), \quad u_{\nu}(p') \rightarrow v_{\nu}(-p_-). \quad (12)$$

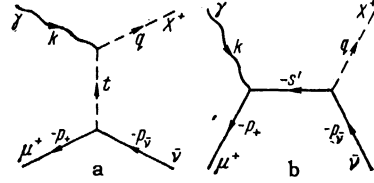


FIG. 2. Feynman diagrams of (II): $k, p, \bar{\nu}, p_+$ and q —4-momenta of the photon, antineutrino, μ^+ meson, and X-meson, respectively; $-s' \equiv t'_2 = -p_+ - k = -p - \bar{\nu} - q$.

The cross section $\sigma_{\gamma+\mu}$, averaged over the photon and μ^+ -meson polarization and summed over the antineutrino and X-meson polarizations is obtained from a formula similar to (6). Integration between the limits ($m^2 \ll \kappa^2$)

$$t^2 |_{min} = -(s'^2 - \kappa^2 - m^2) \cong -(s'^2 - \kappa^2), \\ t^2 |_{max} = \kappa^2 m^2 / s'^2 \cong 0 \quad (13)$$

leads to the following formula for the total cross section of reaction (II):

$$\sigma_{\gamma+\mu} = \frac{\alpha G}{4\sqrt{2}} \left\{ \left[(g-2)^2 + (-g^2 - 8g + 4) \frac{\kappa^2}{s'^2} - 8 \frac{\kappa^4}{s'^4} - 8 \frac{\kappa^6}{s'^6} \right] \right. \\ \times \ln \frac{s'^2}{\kappa^2} + \left[\frac{1}{4} (g-2)^2 + 8(g-1) + \left(-\frac{1}{2} g^2 - 2g + 8 \right) \right. \\ \left. \times \frac{\kappa^2}{s'^2} + \left(\frac{1}{4} g^2 - 5g + 13 \right) \frac{\kappa^4}{s'^4} - 14 \frac{\kappa^6}{s'^6} \right] \right\}. \quad (14)$$

Ebell and Walker^[4] analyzed process (II) directly in the μ^+ -meson rest system.* The expression they obtained for the cross section does not vanish at threshold, however, and is consequently incorrect. It differs from (14) in the numerical coefficients in the second square bracket. The result of Ebell and Walker is therefore correct only at high energies, when the cross section is determined by the logarithmic term.

In the case of large energies ($\kappa^2 \ll s'^2$), going to the limit in (14) and comparing with (11), we obtain

$$\sigma_{\gamma+\nu}(s^2) = 2\sigma_{\gamma+\mu}(s'^2). \quad (15)$$

*To change over to this reference frame it is necessary to put in (14) $s'^2/\kappa^2 = k/k^0$, where $k^0 \approx \kappa^2/2m$ is the photon threshold momentum.

Thus, in this approximation $\sigma_{\gamma+\mu}$ differs from $\sigma_{\gamma+\nu}$ only in the coefficient $1/2$ connected with the averaging over the μ^+ -meson polarization (we assume the incoming neutrino to be longitudinally polarized).

Let us examine in greater detail the reason for this identical dependence of $\sigma_{\gamma+\nu}$ and $\sigma_{\gamma+\mu}$ on s^2 and s'^2 respectively. We recognize that processes (I) and (II) are inverse and can be described by the same matrix element, with the transition from (I) to (II) readily seen to correspond to the substitution $s^2 \rightarrow u^2$, $u^2 \rightarrow s^2$ and $t^2 \rightarrow t'^2$. Diagrams a of both processes are perfectly similar and therefore make identical contributions to the cross section; diagrams b are essentially different and correspond to different denominators in (5). In spite of this, we see that in the high-energy limit the contributions from diagrams b and from their interferences with diagrams a are symmetrical in the variables s^2 and u^2 , i.e., again identical for processes (I) and (II). Furthermore, the limits of integration with respect to t^2 in (6) are also the same at high energies [see (8) and (13)]. The total cross sections therefore satisfy relation (15) obtained above.

3. CROSS SECTIONS OF PROCESSES (A) AND (B)

To calculate the cross sections of reactions (A) and (B) on a heavy nucleus with spin 0 (see Fig. 3) we use the covariant formulation of the Weizsäcker-Williams method^[5]

$$\sigma = -\frac{Z^2\alpha}{2\pi} \int d\omega^2 \frac{dk^2}{k^2} F^2(k^2) \left[1 - \frac{l^2 P'^2}{(lP')^2} \right]^{-1} \times \left\{ a(k^2, \omega^2) \left[1 + \frac{P'^2 (lk)^2}{k^2 (lP')^2} - \frac{(lk)}{(lP')} \right] + b(k^2, \omega^2) \left[(P'^2 - \frac{1}{4} k^2) \frac{(lk)}{(lP')^2} \right] \right\}, \tag{16}$$

where Z —nuclear charge, $b(k^2, \omega^2)$ —unknown function, $a(0, \omega^2)(lk) = \sigma_{\gamma}(w^2)$, and $\sigma_{\gamma}(w^2)$ is given by formulas (9) or (14), in which s^2 and s'^2 are replaced by w^2 .

We confine ourselves henceforth to the following approximation:^[8] 1) $a(k^2, \omega^2)$ differs little from $a(0, \omega^2)$; 2) the main contribution to the integral in (16) is made by the first term in the braces.

For processes (A) and (B) in which muons (but not electrons) participate, these conditions

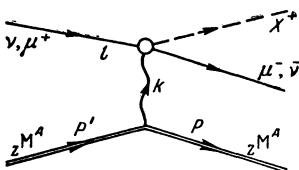


FIG. 3. Feynman diagrams of processes (A) and (B); l , k — 4-momenta of the incoming lepton and Coulomb photon, P' and P — initial and final 4-momenta of the nucleus.

are well satisfied if the energies are not too close to threshold and the momentum transfer to the nucleus is sufficiently small ($|k| \ll M$, where M is the nuclear mass).* In this case expression (16) can be simplified to

$$\sigma = -\frac{Z^2\alpha}{\pi} \int \sigma_{\gamma}(w^2) F^2(k^2) \times \left[\frac{1}{w^2 - k^2 - l^2} + \frac{w^2 - k^2 - l^2}{4E^2 k^2} - \frac{1}{2EM} \right] \frac{dk^2}{k^2} d\omega^2, \tag{17}$$

where E is the energy of the incoming lepton. At large E and when $w^2 \gg k^2$ and l^2 , we obtain from (17) the usual Weizsäcker-Williams formula.

Let us examine a nuclear form factor of the simplest "stepped" type:

$$F(k^2) = \begin{cases} 1 - k^2 < K^2 \\ 0 - k^2 > K^2 \end{cases}, \tag{18}$$

where K —highest value of the virtual-photon momentum, determined by the dimensions of the nucleus ($K = \sqrt{12}/R$, R —rms radius of the nucleus). The limits of integration with respect to w^2 and k^2 are determined from the relation $w^2 = (k+l)^2$, using the conditions $K \ll E$, $K \ll M$, and $l^2 \ll EK$:

$$(w^2/2E)^2 \leq -k^2 \leq K^2, \quad (\kappa + m_l)^2 \leq w^2 \leq 2EK, \tag{19}$$

where m_l is the mass of the produced lepton.

The cross sections of the process (A) calculated from (17) using expression (9) for $\sigma_{\gamma}(w^2)$ leads to integrals that cannot be expressed in terms of elementary functions. We therefore consider the case of very large neutrino energies, when we can approximate $\sigma_{\gamma}(w^2)$ by formula (11).† Integration yields

$$\sigma_{\nu} = \frac{Z^2\alpha^2 G}{6\pi\sqrt{2}} \left\{ (g-2)^2 \ln^3 \xi + \left[-\frac{3}{4}(g-2)^2 + 24(g-1) \right] \ln^2 \xi + O(\ln \xi) \right\}, \tag{20}$$

$$\xi = 2E_{\nu}K/\kappa^2, \quad \ln \xi \gg 1.$$

This result coincides with the cross section obtained by Lee and Yang;^[3] the latter, however, contains a factor $-1/2$ in front of $(g-2)^2 \ln^2 \xi$. We calculated the coefficient $-3/4$ in front of this term in (20) by several independent methods. In addition, the formula with coefficient $-1/2$ leads to a negative σ at energies high enough that the approximation $\ln \xi \gg 1$ is well satisfied and the cross section should be positive.

If the cross section of the process (B) is cal-

*The cross section for the production of the X meson was obtained by Lee and Yang^[3,9] for large $|k|$, when the nucleus does not stay whole.

†The main contribution to the integral in (17) is made by the small w^2 , for which (11) greatly undervalues σ_{γ} ; this approximation is therefore very crude.

culated from (14), then the integration in (17) can be carried through to conclusion and we obtain

$$\begin{aligned} \sigma_\mu = & \frac{Z^2 \alpha^2 G}{12\pi\sqrt{2}} \left\{ (g-2)^2 \ln^3 \eta \right. \\ & \left. + \left[-\frac{3}{4}(g-2)^2 + 24(g-1) \right] \ln^2 \eta + R(\eta) \right\}, \\ R(\eta) = & -\frac{12}{\eta^3} \ln^2 \eta \\ & - \ln \eta \left\{ \left[\frac{15}{2}(g-2)^2 + 132(g-1) + \frac{28}{3} \right] \right. \\ & \left. + \frac{12}{\eta} [(g-2)^2 + 12(g-1) + 4] \right. \\ & \left. + \frac{3}{\eta^2} \left[-\frac{1}{4}(g-2)^2 + 4(g-1) \right] - \frac{32}{3\eta^3} \right\} \\ & + \left\{ \left[\frac{147}{8}(g-2)^2 + 240(g-1) + \frac{266}{9} \right] \right. \\ & \left. + \frac{6}{\eta} [-3(g-2)^2 - 32(g-1) + 4] \right. \\ & \left. + \frac{3}{\eta^2} \left[-\frac{1}{8}(g-2)^2 - 16(g-1) - 30 \right] + \frac{328}{9\eta^3} \right\}, \\ \eta = & \frac{2E_\mu K}{\kappa^2}. \end{aligned} \quad (21)$$

For large μ^+ -meson energies, expression (21) assumes a form analogous to (20), since $R(\eta) = O(\ln \eta)$ when $\ln \eta \gg 1$.

Ebell and Walker^[4] calculated σ_μ using the usual Weizsäcker-Williams formula. As pointed out above (Sec. 2) their expression for $\sigma_{\gamma+\mu}$ is valid only at very high energies. Consequently only the principal term with $\ln^3 \eta$ is correct in the result of Ebell and Walker.

4. CROSS SECTIONS OF THE PROCESSES (A) AND (B) FOR THE NUCLEUS ${}_{26}\text{Fe}^{56}$

To obtain cross sections for comparison with the results of future experiments, we consider the processes (A) and (B) in the ${}_{26}\text{Fe}^{56}$ nucleus ($M = 52.1$ BeV) and use for the form factor an expression that agrees with the experimental charge distribution

$$F(k^2) = \int \frac{\rho_0 \exp(ikr) d\tau}{1 + \exp[(r-c)/z]}, \quad \rho_0^{-1} = \int \frac{d\tau}{1 + \exp[(r-c)/z]}, \quad (22)$$

where $k \equiv \sqrt{-k^2}$, $c = 4.05 F$, and $z = 0.568 F$.^[10] Integrating, we obtain

$$F(k^2) \approx \frac{3\pi z}{(c^2 + \pi^2 z^2) k \operatorname{sh}(\pi k z)} \left[-\cos(kc) + \frac{\pi z \sin(kc)}{c \operatorname{th}(\pi k z)} \right]. \quad (23)^*$$

The limits of w^2 and k^2 (see also ^[8]) are now determined only by the kinematics of the processes and are equal to †

*sh = sinh; th = tanh.

†We note that in the case of process (A) the expression given for ε_\pm^2 corresponds exactly to the vanishing of the square bracket in (17).

$$(\kappa + m_l)^2 \leq \omega^2 \leq M^2 (\sqrt{1 + 2E/M} - 1)^2,$$

$$\varepsilon_-^2 \leq -k^2 \leq \varepsilon_+^2,$$

$$\varepsilon_\pm^2 \cong \left(1 + \frac{2E}{M}\right)^{-1} \left\{ 2E^2 \left[1 \pm \sqrt{1 + \frac{\omega^4}{4E^2 M^2} - \frac{\omega^2}{E^2} \left(1 + \frac{E}{M}\right)} \right] - \omega^2 \left(1 + \frac{E}{M}\right) \right\}. \quad (24)$$

The integration in (17) was by numerical means using cross sections (9)–(10) and (14) for the case $g = 1$ and for three X-meson masses, viz. $0.6 m_p$, $1.0 m_p$ and $1.4 m_p$.

The results obtained for σ_ν/Z and σ_μ/Z are plotted in Figs. 4 and 5. It should be noted that

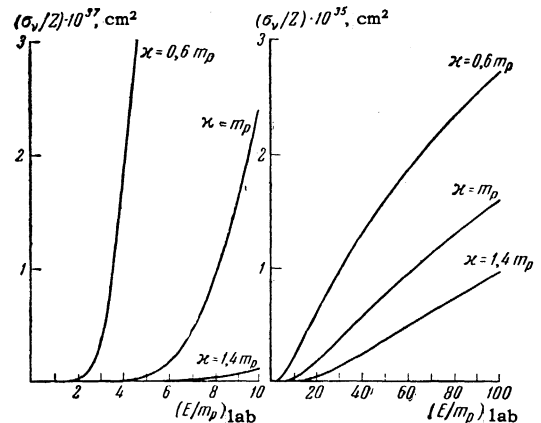


FIG. 4. Dependence of the cross section of the process $\nu + \text{Fe} \rightarrow X^+ + \mu^- + \text{Fe}$ (A) on the neutrino energy; $g = 1$.

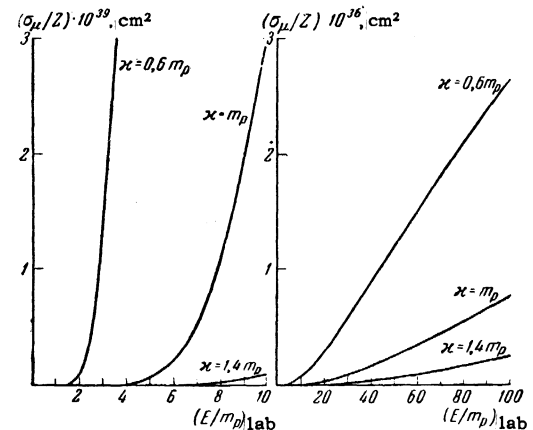


FIG. 5. Dependence of the cross section of the process $\mu^+ + \text{Fe} \rightarrow X^+ + \bar{\nu} + \text{Fe}$ (B) on the μ^+ meson energy; $g = 1$.

the curves for σ_ν/Z are much steeper near threshold than the curves in Lee's Geneva Conference paper.^[9] The latter, however, does not mention the calculation procedure, so that we are unable to explain this discrepancy.

The authors are sincerely grateful to L. B. Okun' for suggesting the problem and for continuous interest in the work and are indebted to I. Yu. Kobzarev, K. A. Ter-Martirosyan and E. P. Sha-

balin for discussions. We also take this opportunity to thank I. G. Kristi for the numerical integration.

Note added in proof (April 12, 1962). It is seen from a recently published paper by Lee, Markstein, and Yang^[11] that the σ_ν/Z plots for energies up to ~ 6 BeV, given in [9], were obtained by numerical integration without the use of the Weizsäcker-Williams method. Thus, the difference noted in the behavior of σ_ν/Z at threshold is due essentially to the poor applicability of approximations 1) and 2) (see Sec. 3) at these energies. In addition, the form factor used in [11]

$$F(k^2) = (1 + k^2 a^2/12)^{-2}, \quad a = \sqrt{3/5} \cdot 1.3 A^{1/3} F,$$

leads to larger values of σ_ν than the form factor (23). We note that this difference, of course, disappears with increasing energy E .

¹H. Yukawa, *Revs. Modern Phys.* **21**, 474 (1949).
S. Ogawa, *Progr. Theor. Phys.* **15**, 487 (1956).
T. D. Lee and C. N. Yang, *Phys. Rev.* **108**, 1611 (1957), *J. Schwinger, Ann. Phys.* **2**, 407 (1957).
R. P. Feynman and M. Gell-Mann, *Phys. Rev.* **109**, 193 (1958), E. C. G. Sudarshan and R. E. Marshak, *Phys. Rev.* **109**, 1860 (1958).

²B. M. Pontecorvo and R. M. Ryndin, Ninth

International Conference on High-energy Physics, Kiev, (1959).

³T. D. Lee, *Ann. Intern. Conference on High Energy Physics at Rochester*, (1960).

⁴M. E. Ebell and W. D. Walker, *Phys. Rev.* **122**, 1639 (1961).

⁵Gribov, Kolkunov, Okun', and Shekhter, *JETP* **41**, 1839 (1961), *Soviet Phys. JETP* **14**, 1308 (1962).

⁶T. D. Lee and C. N. Yang, *Phys. Rev. Lett.* **4**, 307 (1960); *Phys. Rev.* **119**, 1410 (1960).

⁷W. Pauli, *Relativistic Field Theories of Elementary Particles (Russ. Transl.)*. *Revs. Modern Phys.* **13**, 203 (1941). R. Feynman, *Phys. Rev.* **76**, 769 (1949).

⁸M. A. Kozhushner and E. P. Shabalin, *JETP* **41**, 949 (1961), *Soviet Phys. JETP* **14**, 676 (1962).

⁹T. D. Lee, *Intern. Conf. on Theor. Aspects of Very High Energy Phenomena, Geneva*, (1961).

¹⁰Hahn, Hofstadter, and Ravenhall, *Phys. Rev.* **105**, 1353 (1957).

¹¹Lee, Markstein, and Yang, *Phys. Rev. Lett.* **7**, 429 (1961).

Translated by J. G. Adashko
207